Centrum voor Wiskunde en Informatica
Centre for Mathematics and Computer Science

J. Molenaar

Non-linear multigrid in 2-D semiconductor device simulation:
the zero current case

Department of Numerical Mathematics Report NM-R8917 November

The Centre for Mathematics and Computer Science is a research institute of the Stichting Mathematisch Centrum, which was founded on February 11, 1946, as a nonprofit institution aiming at the promotion of mathematics, computer science, and their applications. It is sponsored by the Dutch Government through the Netherlands Organization for the Advancement of Research (N.W.O.).

Non-linear Multigrid in 2-D Semiconductor Device Simulation: the Zero Current Case

J. Molenaar
Centre for Mathematics and Computer Science
P.O. Box 4079, 1009 AB Amsterdam, The Netherlands

The non-linear Poisson equation, encountered in semiconductor device simulation, is discretized by the mixed finite element method. Two non-linear relaxation methods are presented to solve the discretized equations; both minimize appropriate functionals. One of them, a 5-point Vanka-type relaxation is used in a multigrid algorithm. Numerical results are given for simple diode problems.

1980 Mathematics Subject Classification: 65N20, 65H190
Keywords & Phrases: semiconductor equations, multigrid methods

1. Introduction

A steady state semiconductor device can be modelled by a non-linear Poisson equation, if it is assumed that the electron and hole current densities vanish (see [1]). A simplified version of this equation is introduced in section 2.

In section 3 the Poisson equation is discretized by the mixed finite element method for rectangular grids. The continuous and discrete problems can be reformulated as minimization of appropriate functionals (section 4).

Schmidt and Jacobs [2] constructed a superbox-relaxation method for linear problems (with Neumann boundary conditions), based upon a variational principle. We extend their algorithm to the non-linear case, and to more general boundary conditions (section 5). It is shown that also the Vanka-relaxation can be seen as minimization of a functional, provided that the discrete equations are lumped. The usefulness of these two relaxation methods for semiconductor device simulation is examined by numerical experiments (section 6). In section 7 we show results of a multigrid method using Vanka-relaxation for a simple test problem. In the final section conclusions are summarized.

2. The problem

We consider Poisson's equation for the electrostatic potential ψ in a semiconductor device, given by

$$-\operatorname{div}(\epsilon \operatorname{grad} \psi) = f(\psi)+D, \tag{2.1}$$

with ϵ, the positive (constant) permittivity, and D, the known dope function.

The total charge density of electrons and holes, is given by

$$f(\psi) = -2n_i q \sinh(\alpha\psi), \tag{2.2}$$

where $n_i q$, the intrinsic charge density, and α^{-1}, the thermal voltage are constants.

At the contacts of the device, space charge neutrality is required:

$$f(\psi_D)+D = 0. \tag{2.3}$$

In this paper we take (2.1) as point of departure, $f(\psi)$ is an arbitrary analytical function, and it is required that

$$-\frac{df(\psi)}{d\psi} > 0. \tag{2.4}$$

Report NM-R8917
Centre for Mathematics and Computer Science
P.O. Box 4079, 1009 AB Amsterdam, The Netherlands

The domain Ω is bounded in $\mathbf{R}^2$; the boundary conditions are either homogeneous Neumann or Dirichlet on parts of the boundary

$$\psi(\mathbf{x}) = g(\mathbf{x}), \quad x \in \delta\Omega_D, \tag{2.5}$$

$$\frac{\partial \psi}{\partial n} \cdot \mathbf{n} = 0, \qquad x \in \delta\Omega_N, \tag{2.6}$$

$$\delta\Omega_D \cup \delta\Omega_N = \delta\Omega, \tag{2.7}$$

$$\delta\Omega_D \cap \delta\Omega_N = \varnothing. \tag{2.8}$$

3. Mixed finite element discretization

The mixed finite element method is used to derive discrete equations for (2.1). For an abstract treatment of the linear case, see Girault-Raviart [3].

We start by writing (2.1) as two first order equations

$$\left.\begin{aligned} \operatorname{div} \mathbf{u} - f(\psi) &= D \\ \mathbf{u} + \epsilon \operatorname{grad} \psi &= 0 \end{aligned}\right\} \quad \text{on } \Omega, \tag{3.1a, 3.1b}$$

$$\mathbf{u} \cdot \mathbf{n} = 0, \qquad \text{on } \delta\Omega_N, \tag{3.1c}$$

$$\psi = g, \qquad \text{on } \delta\Omega_D, \tag{3.1d}$$

with $\mathbf{u}$ as a new variable.

Let $L_2(\Omega)$ be the space of square integrable functions on Ω with inner product

$$(\psi, \phi)_{L_2} = \int_\Omega \phi\psi \, d\Omega, \tag{3.2}$$

and the induced norm $\|\cdot\|_{L_2}$.

$H(\operatorname{div}, \Omega)$ is defined by

$$H(\operatorname{div}, \Omega) = \{\mathbf{u} \mid \mathbf{u} \in (L_2(\Omega))^2, \operatorname{div} \mathbf{u} \in L_2(\Omega), \mathbf{u} \cdot \mathbf{n} = 0 \text{ on } \delta\Omega_N\}, \tag{3.3}$$

with norm

$$\|\mathbf{u}\|_H^2 = \|\mathbf{u}\|_{(L_2)^2}^2 + \|\operatorname{div} \mathbf{u}\|_{L_2}^2. \tag{3.4}$$

With introduction of the product space $\Lambda = L_2(\Omega) \times H(\operatorname{div}, \Omega)$, the weak formulation of (3.1) is find $(\psi, \mathbf{u}) \in \Lambda$, such that $\forall (\phi, \mathbf{v}) \in \Lambda$

$$(\operatorname{div} \mathbf{u} - f(\psi), \phi) = (D, \phi), \tag{3.5a}$$

$$\epsilon^{-1}(\mathbf{u}, \mathbf{v}) - (\psi, \operatorname{div} \mathbf{v}) = -\langle g, \mathbf{v} \rangle_{\delta\Omega}, \tag{3.5b}$$

$$\text{with } \langle g, \mathbf{v} \rangle_{\delta\Omega} = \int_{\delta\Omega} g \mathbf{v} \cdot d\mathbf{n} \tag{3.6}$$

In order to discretize (3.5) we take lowest order Raviart-Thomas elements on grid rectangles as basis for the approximating subspaces.

On every block Ω_i of the grid, define the indicator function $\epsilon_i \in L_2(\Omega)$

$$\epsilon_i(\mathbf{x}) = \begin{cases} 0, & \mathbf{x} \notin \Omega_i, \\ 1, & \mathbf{x} \in \Omega_i. \end{cases} \tag{3.7}$$

For every side E_j of some block Ω_i, not part of the Neumann boundary, introduce $\mathbf{e}_j \in H(\operatorname{div}, \Omega)$ by

$$\mathbf{e}_j(\mathbf{x}) = \begin{bmatrix} \alpha + \beta x \\ \gamma + \delta y \end{bmatrix}, \tag{3.8}$$

with $(\alpha, \beta, \gamma, \delta)$ such that

$$\mathbf{e}_j \cdot \mathbf{e}_k = \delta_{jk}, \text{ on interfaces } E_k. \tag{3.9}$$

The spaces spanned by $\{\epsilon_i\}$ and $\{\mathbf{e}_j\}$ are called $L_2^d(\Omega)$ and $H^d(\text{div}, \Omega)$, respectively. Also, there is the product space $\Lambda^d = L_2^d(\Omega) \times H^d(\text{div}, \Omega)$. The discrete approximation of the unknowns is

$$\psi^d = \sum_i \psi_i \, \epsilon_i, \tag{3.10}$$

$$\mathbf{u}^d = \sum_j u_j \, \mathbf{e}_j. \tag{3.11}$$

Summation in (3.10) is over all blocks Ω_i, and in (3.11) over all sides E_j of blocks ($E_j \not\subset \delta\Omega_N$).

REMARK 1. The Neumann boundary conditions are automatically satisfied by functions in $H^d(\text{div}, \Omega)$.

REMARK 2. ψ is approximated by a piecewise constant function, $\mathbf{u}$ by a piecewise linear vector function, of which the normal components are continuous at block interfaces.

The selection of the discretization method and the set of basis functions is based on the expectation that $\mathbf{u}$ will be much smoother than ψ in semiconductor device simulation.

To discretize (3.5a-3.5b) take $\phi = \epsilon_i$ and $\mathbf{v} = \mathbf{e}_j$, respectively, and integrate in order to obtain

$$\sum_j u_j d_{ji} - f_i(\psi^d) = D_i \tag{3.12a}$$

and

$$\sum_k u_k w_{kj} - \sum_i d_{ji} \psi_i = -g_j. \tag{3.12b}$$

D_i, f_i and g_j are defined by

$$D_i = \int_{\Omega_i} D \, d\Omega, \tag{3.13}$$

$$f_i = \int_{\Omega_i} f(\psi^d) \, d\Omega \tag{3.14}$$

and

$$g_j = \int_{\delta\Omega_D} g \mathbf{e}_j \cdot d\mathbf{n}. \tag{3.15}$$

The elements of the matrices w_{kj} and d_{ji} are given by

$$w_{kj} = \epsilon^{-1} \int_{\Omega} \mathbf{e}_k \cdot \mathbf{e}_j \, d\Omega \tag{3.16}$$

and

$$d_{ji} = \begin{cases} +h_j, & \text{if } E_j \text{ is a positive side of } \Omega_i, \\ -h_j, & \text{if } E_j \text{ is a negative side of } \Omega_i, \\ 0, & \text{otherwise,} \end{cases} \tag{3.17}$$

with h_j the length of side E_j. Notice that (3.12a) implies that the conservation law is satisfied for every block Ω_i. Equation (3.12b) is obtained for all interfaces E_j not part of the Neumann boundary.

It is known that with the above MFEM-discretization the Jacobian of the whole system is not a M-matrix. A remedy is to use lumping, or, equivalently to use a suitable quadrature rule for the evaluation of w_{kj}. If we apply the trapezoidal rule w_{kj} is approximated by

$$\epsilon^{-1}\int_{\Omega_i}\mathbf{e}_k\cdot\mathbf{e}_j\,d\Omega \approx \epsilon^{-1}\frac{a_i}{4}\sum_{v=1,4}\mathbf{e}_k(\mathbf{x}_v)\cdot\mathbf{e}_j(\mathbf{x}_v), \tag{3.18}$$

where the summation is over the vertices of Ω_i (with area a_i). This quadrature approximates w_{kj} by a diagonal matrix.

4. Variational formulations

In this section two variational formulations for (3.5) are derived. For the linear case and Neumann boundary conditions Schmidt and Jacobs [2] showed that the solution of (3.5) minimizes a quadratic functional, with (3.5a) as an auxiliarly condition. This idea is extended to non-linear problems and more general boundary conditions.

On the other hand, it is also possible to define a minimizing functional for (3.5), when (3.5b) is used as auxilary condition.

We start by defining subspaces of Λ in which the minima are to be found

$$\Lambda_a = \{(\psi, \mathbf{u})\in\Lambda \mid (\operatorname{div}\mathbf{u}-f(\psi),\phi)=(D,\phi), \quad \forall\phi\in L_2(\Omega)\} \tag{4.1a}$$

and

$$\Lambda_b = \{(\psi, \mathbf{u})\in\Lambda \mid \frac{1}{\epsilon}(\mathbf{u},\mathbf{v})-(\psi,\operatorname{div}\mathbf{v})=-\langle g,\mathbf{v}\rangle_{\delta\Omega}, \quad \forall\in H(\operatorname{div},\Omega)\}. \tag{4.1b}$$

The minimizing functionals are defined by

$$F_a(\phi, \mathbf{v}) = \int_\Omega (\frac{\mathbf{v}^2}{2\epsilon} + R_a(\phi))d\Omega + \langle g, \mathbf{v}\rangle_{\delta\Omega} \tag{4.2a}$$

and

$$F_b(\phi, \mathbf{v}) = \int_\Omega (\frac{\mathbf{v}^2}{2\epsilon} + R_b(\phi)-D\phi)d\Omega, \tag{4.2b}$$

with

$$\frac{dR_a}{d\phi} = -\phi\frac{df(\phi)}{d\phi} \tag{4.3a}$$

and

$$\frac{dR_b}{d\phi} = -f(\phi). \tag{4.3b}$$

The variational principles are now stated in two theorems.

Theorem 1. *$(\psi, \mathbf{u})$ is a solution of (3.5) if and only if F_a has a local minimum in Λ_a for $(\psi, \mathbf{u})$.*

Proof. Let $(\psi, \mathbf{u})$ be the solution of (3.5) then $(\psi, \mathbf{u})\in\Lambda_a$.
If $(\psi+\lambda\phi, \mathbf{u}+\lambda\,\mathbf{v})\in\Lambda_a$ in the neighbourhood of $(\psi, \mathbf{u})$, then, using a Taylor expansion for $0<\lambda\ll 1$ and (4.1a), we obtain

$$(\operatorname{div}(\lambda\,\mathbf{v}),\,\psi) = (f(\psi+\lambda\phi)-f(\psi),\,\psi) = (\frac{df}{d\psi}(\lambda\phi) + \frac{d^2f}{d\psi^2}\frac{(\lambda\phi)^2}{2},\psi) + O((\lambda\phi)^3).$$

A Taylor expansion for R_a yields

$$\begin{aligned}(R_a(\psi+\lambda\phi)-R_a(\psi),1) = (\frac{dR_a}{d\psi},\lambda\phi) + (\frac{d^2R}{d\psi^2},\frac{(\lambda\phi)^2}{2}) + O((\lambda\phi)^3)\\ - (\psi\frac{df}{d\psi},\lambda\phi)-(\frac{df}{d\psi}+\psi\frac{d^2f}{d\psi^2},\frac{(\lambda\phi)^2}{2}) + O((\lambda\phi)^3)\end{aligned}$$

$$- (\mathrm{div}(\lambda\, \mathbf{v}),\, \psi) - (\frac{df}{d\psi},\, \frac{(\lambda\phi)^2}{2}) + O((\lambda\phi)^3). \tag{4.5}$$

Using (4.5) and (4.2a)

$$F_a(\psi+\lambda\phi, \mathbf{u}+\lambda\, \mathbf{v}) - F_a(\psi, \mathbf{u}) = \frac{1}{\epsilon}(\mathbf{u}, \lambda\, \mathbf{v}) + \frac{1}{2\epsilon}(\lambda\, \mathbf{v}, \lambda\, \mathbf{v}) + (R_a(\psi+\lambda\phi) - R_a(\psi), 1)$$

$$+ \langle g, \lambda\, \mathbf{v}\rangle_{\delta\Omega} = \frac{1}{\epsilon}(\mathbf{u}, \lambda\, \mathbf{v}) - (\mathrm{div}(\lambda\, \mathbf{v}),\, \psi) + \langle g, \lambda\, \mathbf{v}\rangle_{\delta\Omega}$$

$$+ \frac{1}{2\epsilon}(\lambda\, \mathbf{v}, \lambda\, \mathbf{v}) - (\frac{df}{d\psi},\, \frac{(\lambda\phi)^2}{2}) + O((\lambda\phi)^3).$$

Due to (3.5b) and (2.4) F_a has a local minimum in Λ_a. On the other hand, if $(\psi, \mathbf{u}) \in \Lambda_a$, and $F_a(\psi, \mathbf{u})$ has a local minimum for all perturbations $(\lambda\phi, \lambda\, \mathbf{v})$ such that $(\psi+\lambda\phi, \mathbf{u}+\lambda\, \mathbf{v}) \in \Lambda_a$, then

$$\frac{1}{\epsilon}(u, \lambda\, \mathbf{v}) - (\psi, \mathrm{div}\lambda\, \mathbf{v}) + \langle g, \lambda\, \mathbf{v}\rangle_{\delta\Omega} = 0$$

for all $\mathbf{v} \in H(\mathrm{div}, \Omega)$, and hence (3.5b) holds. □

THEOREM 2. *$(\psi, \mathbf{u})$ is a solution of (3.5) if and only if F_b has a local minimum in Λ_b for $(\psi, \mathbf{u})$.*

PROOF. Let $(\psi, \mathbf{u})$ be the solution of (3.5) then $(\psi, \mathbf{u}) \in \Lambda_b$.
If $(\psi+\lambda\phi, \mathbf{u}+\lambda\, \mathbf{v}) \in \Lambda_b$ in the neighbourhood of $(\psi, \mathbf{u})$, then (4.1b) implies

$$\frac{1}{\epsilon}(\lambda\, \mathbf{v}, \mathbf{u}) - (\lambda\phi, \mathrm{div}\, \mathbf{u}) = 0. \tag{4.7}$$

Using (4.2b) and (4.7) yields

$$F_b(\psi+\lambda\phi, \mathbf{u}+\lambda\, \mathbf{v}) - F_b(\psi, \mathbf{u}) = \frac{1}{\epsilon}(\mathbf{u}, \lambda\, \mathbf{v}) + \frac{1}{2\epsilon}(\lambda\, \mathbf{v}, \lambda\, \mathbf{v}) + (R_b(\psi+\lambda\phi) - R_b(\psi), 1)$$

$$- (D, \lambda\phi) = (\mathrm{div}\, \mathbf{u}, \lambda\phi) - (f(\psi), \lambda\phi) - (D, \lambda\phi)$$

$$+ \frac{1}{2\epsilon}(\lambda\, \mathbf{v}, \lambda\, \mathbf{v}) - (\frac{df}{d\psi},\, \frac{(\lambda\phi)^2}{2}) + O((\lambda\phi)^3). \tag{4.8}$$

This shows that F_b has a local minimum in Λ_b for $(\psi, \mathbf{u})$. It also shows that, if F_b has a local minimum, then (3.5a) must hold. □

Like the continuous case, the problem of solving (3.12) can be seen as minimization, viz. of

$$F_a^d(\psi^d, \mathbf{u}^d) = \int (\frac{1}{2\epsilon}\mathbf{u}^d \cdot \mathbf{u}^d + R_a(\psi^d))d\Omega + \langle g, \mathbf{u}^d\rangle_{\delta\Omega}$$

$$= \frac{1}{2}\sum_{kj} u_k\, w_k\, u_j + (R_a(\psi^d), 1) + \sum_j g_j u_j \tag{4.9a}$$

and

$$F_b^d(\psi^d, \mathbf{u}^d) = \int (\frac{1}{2\epsilon}\mathbf{u}^d \cdot \mathbf{u}^d + R_b(\psi^d) - D\psi^d)d\Omega$$

$$= \frac{1}{2}\sum_{kj} u_k\, w_{kj}\, u_j + (R_b(\psi^d), 1) - \sum_i D_i\, \psi_i^d, \tag{4.9b}$$

in respectively the subspaces

$$\Lambda_a^d = \{(\psi^d, \mathbf{u}^d) \in \Lambda^d \mid \sum_j u_j d_{ji} - f_i(\psi^d) = D_i,\ \forall i\} \tag{4.10a}$$

and

$$\Lambda_b^d = \{(\psi^d, \mathbf{u}^d) \in \Lambda^d \mid \sum_k u_k w_{kj} - \sum_i d_{ji}\psi_i = -g_j, \ \forall j\}. \tag{4.10b}$$

Discrete versions of theorem 1 and 2 can now be stated.

THEOREM 3. *$(\psi^d, \mathbf{u}^d)$ is a solution of (3.12) if and only if F_a^d has a local minimum in Λ_a^d for $(\psi^d, \mathbf{u}^d)$.*

PROOF. Let $(\psi^d, \mathbf{u}^d)$, $(\psi^d + \lambda\phi^d, \mathbf{u}^d + \lambda\, \mathbf{v}^d) \in \Lambda_a^d$ then

$$\sum_j \lambda v_j d_{ji} - (f_i(\psi^d + \lambda\phi^d) - f_i(\psi^d)) = 0, \quad \forall i. \tag{4.11}$$

Using (4.9a), (4.5) and (4.11) yields $(0 < \lambda \ll 1)$

$$\begin{aligned} F_a^d(\psi^d + \lambda\phi^d, \mathbf{u}^d + \lambda\, \mathbf{v}^d) - F_a^d(\psi^a, \mathbf{u}^d) &= \sum_{kj} u_k w_{kj} \lambda v_j + \sum_i \int_{\Omega_i} (R_a(\psi^d + \lambda\phi^d) - R(\psi^d)) d\Omega \\ &+ \sum_j g_j \lambda v_j + \frac{\lambda^2}{2} \sum_{kj} v_k w_{kj} v_j = \lambda \sum_j \Big(\sum_k u_k w_{kj} - \sum_i \psi_i d_{ji} + g_j\Big) v_j \\ &+ \frac{\lambda^2}{2} \sum_{kj} v_k w_{kj} v_j - \frac{\lambda^2}{2} \sum_i \Big(\phi_i^2 \int_{\Omega_i} \frac{df}{d\psi}\, d\Omega\Big) + O((\lambda\phi)^3). \end{aligned} \tag{4.12}$$

Together with (2.4) and the positive definiteness of the matrix w_{kj}, (4.12) proves the theorem. □

THEOREM 4. *$(\psi^d, \mathbf{u}^d)$ is a solution of (3.12) if and only if F_b^d has a local minimum in Λ_b^d for $(\psi^d, \mathbf{u}^d)$.*

PROOF. Let $(\psi^d, \mathbf{u}^d)$, $(\psi^d + \lambda\phi^d, \mathbf{u}^d + \lambda\, \mathbf{v}^d) \in \Lambda_b^d$, then

$$\sum_k v_k w_{kj} - \sum_i d_{ji}\, \phi_i = 0. \tag{4.13}$$

Using (4.9b), (4.13) and (4.3b), we find

$$\begin{aligned} F_b^d(\psi^d + \lambda\phi^d, \mathbf{u}^d + \lambda\, \mathbf{v}^d) - F^d(\psi^d, \mathbf{u}^d) &= \sum_{kj} u_k\, w_{kj} \lambda v_j + \sum_i \int_{\Omega_i} (R_b(\psi^d + \lambda\phi^d) - R_b(\psi^d)) d\Omega \\ -\lambda \sum_i D_i \phi_i + \frac{\lambda^2}{2} \sum_{kj} v_k w_{kj} v_j &= \sum_{kj} u_k w_{kj} \lambda v_j + \sum_i \lambda(-f_i - D_i)\phi_i - \sum_i \Big(\frac{(\lambda\phi_i)^2}{2} \int_{\Omega_i} \frac{df}{d\psi} d\Omega\Big) \\ + \frac{\lambda^2}{2} \sum_{kj} v_k w_k v_j + O((\lambda\phi)^3) &= \sum_i \lambda\phi_i \Big(\sum_j u_j d_{ji} - f_i - D_i\Big) - \sum_i \frac{(\lambda\phi_i)^2}{2} \int_{\Omega_i} \frac{df}{d\psi} d\Omega \\ + \frac{\lambda^2}{2} \sum_{kj} v_k w_{kj} v_j + O((\lambda\phi)^3). \end{aligned} \tag{4.14}$$

As before, (4.14) proves the theorem. □

5. RELAXATION METHODS

The two variational formulations of the discrete equations can be used to construct two non-linear relaxation methods. The superbox-relaxation (section 5.1) is similar to a method developed by SCHMIDT and JACOBS [2]. For this relaxation, the functional $F_a^d(\psi, \mathbf{u})$ is minimized in small relaxation subspaces, while (3.12a) remains valid everywhere in Ω. Provided that the lumped form of the equations is used the 5-point Vanka-relaxation [4] (section 5.2) can be seen as minimization of $F_b^d(\psi, \mathbf{u})$ over Λ_b^d.

5.1. Superbox-relaxation

Extending Schmidt and Jacobs' approach for Dirichlet boundary conditions and for $f \neq 0$, the following relaxation subdomains in Ω are defined:

i. four blocks with a common vertex (fig. 5.1),
ii. two blocks with a common vertex, on the Dirichlet boundary (fig. 5.2),
iii. a corner block, where two Dirichlet boundaries meet (fig. 5.3).

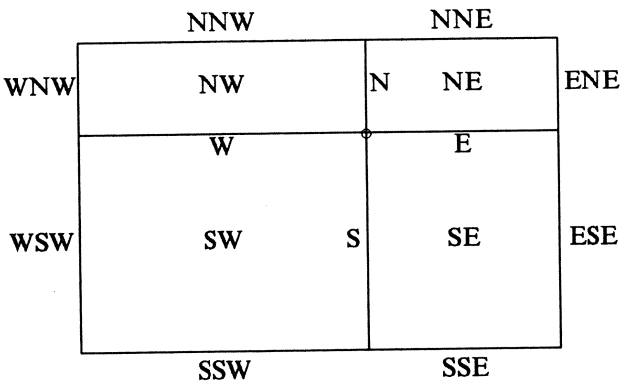

FIGURE 5.1.

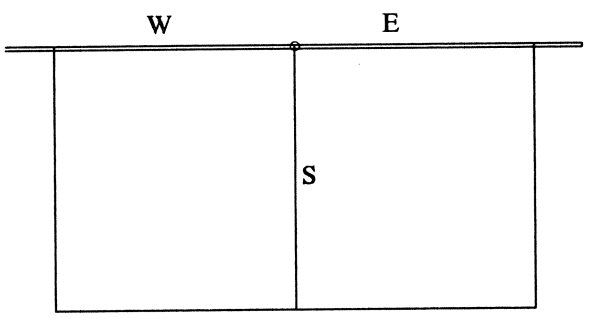

FIGURE 5.2.

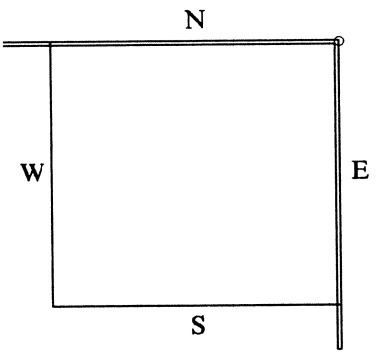

FIGURE 5.3.

In the first case F_a^d is minimized over the degrees of freedom inside the four blocks, whereas the fluxes through the external interfaces $u_{NNE}, \ldots, u_{NNW}$ are kept fixed; thus ensuring that (3.12a) remains true outside the relaxation subdomain. Minimizing F_a^d means solving (3.12a) and (3.12b) inside the subdomain. This leads to four equations (3.12a) for the blocks, and four equations (3.12b) for the internal interfaces. This yields a set of 8 equations for the unknowns $u_N, \ldots, u_W$, and $\psi_{NE}, \ldots, \psi_{NW}$.

Because (3.12b) is linear, the fluxes u are easily eliminated, leaving four non-linear equations for ψ. This set of equations is solved by Newton iteration.

The Jacobian matrix J can be written as the sum of a diagonal matrix and a singular matrix

$$J = \begin{bmatrix} \hbar_N+\hbar_E & -\hbar_E & 0 & -\hbar_N \\ -\hbar_E & \hbar_S+\hbar_E & \hbar_S & 0 \\ 0 & -\hbar_S & \hbar_S+\hbar_W & -\hbar_W \\ -\hbar_N & 0 & -\hbar_W & \hbar_N+\hbar_W \end{bmatrix}$$

$$+ \begin{bmatrix} -f'_{NE}a_{NE} & & & 0 \\ & -f'_{SE}a_{SE} & & \\ & & -f'_{SW}a_{SW} & \\ 0 & & & -f'_{NW}a_{NW} \end{bmatrix}, \tag{5.1.1}$$

where

$$f'_{NE} = \frac{df}{d\psi}|_{\psi_{NE}}, \text{ etc.},$$

$$a_{NE} = h_N h_E, \text{ etc.},$$

and

$$\hbar_N = \frac{3\epsilon h_N}{h_E+h_W}, \text{ etc.},$$

in the non-lumped case or

$$\hbar_N = \frac{2\epsilon h_N}{h_E+h_W}, \text{ etc.},$$

in the lumped case. The Jacobian is symmetric and diagonally dominant (due to (2.4)), but this dominance gets weaker if the meshsize decreases. Numerically, the Jacobian can become singular. In the numerical experiments given in section 6 we used as a criterion

$$\sum_{i=1,4} |a_i f'_i| < 10^{-9}. \tag{5.1.2}$$

In this case the right-hand side is projected onto the range of the columns of J and the solution of the resulting system is determined for which

$$\psi_{NE} + \psi_{SE} + \psi_{SW} + \psi_{NW} = \text{constant}. \tag{5.1.3}$$

This is similar to the way Schmidt and Jacobs [2] treat the special case $f \equiv 0$.

If a relaxation subdomain consists of two blocks only, this can be seen as a special case of the previous one. E.g. in the case given in fig. 5.2, meshsize h_N equals zero, and ψ_{NE} and ψ_{NW} are prescribed by the boundary conditions. We replace the equations for ψ_{NE} and ψ_{NW} accordingly, and eliminate the fluxes at the Dirichlet boundaries. The Jacobian matrix of this system is non-symmetric and non-singular.

The third case (fig. 5.3) is quite simple. After elimination of the fluxes at the Dirichlet boundaries, there is only one equation for ψ, which is solved by Newton iteration.

After having minimized the functional inside a relaxation subdomain, the newly calculated values are substituted, and we proceed to a next subspace. This is done in some order equivalent with lexicographical ordering. Thus we obtain a Gauss-Seidel type of relaxation. Since, by the equations, all blocks are only related with their direct neighbours, the Gauss-Seidel sweeps can be identified by their diagonal direction (as in the case for simple 5-point schemes). So, we identify the different sweeps of Gauss-Seidel relaxation by $NE-SW$ etc., and symmetric Gauss-Seidel sweeps by $NE-SW-NE$ etc.

5.2. Vanka-type relaxation

In the 5-point Vanka-relaxation the relaxation subdomain consists of 5 blocks (see fig. 5.4). In the step of the relaxation procedure that corresponds with cell C, F_b^d is minimized with $\psi_C, u_N, \ldots, u_W$ as degrees of freedom; all other variables are kept fixed.

Notice that, if the equations are lumped, (3.12b) gives a relation between u at interface E_j and ψ_i in the two neighbouring blocks; so changing ψ_C only affects $u_N, \ldots, u_W$. Minimizing F_b^d in the subspace, means solving one equation (3.12a) and four equations (3.12b). Hence, after relaxation in the subdomain, (3.12b) still holds everywhere in Ω. Again Newton iteration is used to solve this nonlinear system of 5 equations. We took a straightforward approach with respect to the boundary conditions. Neumann boundaries are treated by replacing the equation (3.12b) by

$$u_{\text{Neumann}} = 0. \tag{5.2.1}$$

Dirichlet boundary conditions are handled by introduction of dummy blocks with zero area at the boundary.

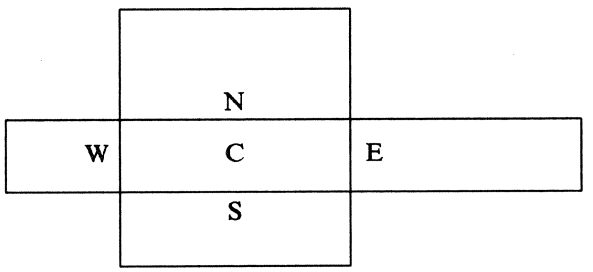

FIGURE 5.4. Relaxation subdomain for Vanka-relaxation

6. NUMERICAL EXPERIMENTS

6.1. A linear problem

In this section we first consider a simple boundary value problem, defined on the unit square $\Omega=[0,1]\times[0,1]$

$$\begin{aligned} -\text{div}(\text{grad}\,\psi) + \lambda^2\psi &= 0, \quad \text{on } \Omega, \\ \psi_D &= y, \quad y = 0 \vee y = 1, \\ \mathbf{u}\cdot\mathbf{n} &= 0, \quad x = 0 \vee x = 1, \end{aligned} \tag{6.1}$$

with λ a constant parameter. The functionals F^d are given by (4.9) with

$$\frac{dR_a}{d\psi} = \frac{dR_b}{d\psi} = \lambda^2\psi. \tag{6.2}$$

The exact solution for ψ is

$$\psi(x,y) = \frac{\sinh(\lambda y)}{\sinh(\lambda)}. \tag{6.3}$$

The cases that large variations in ψ result in small variations of $F^d(\psi,\mathbf{u})$ are of special interest; consider the case $\lambda=0$. If we take $\psi=0$, $\mathbf{u}=0$, as starting values, the superbox-relaxation fails to converge on a 2×2 grid (see fig. 6.1).

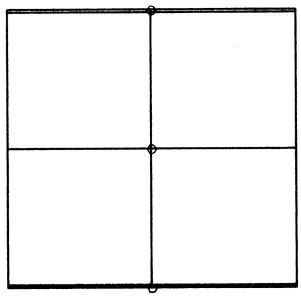

FIGURE 6.1. Superbox relaxation on 2×2 grid.

This can be seen as follows. If we take any of the three relaxations subdomains the fixed fluxes through the external interfaces are zero. Due to (3.12a) and the symmetry of the problem, the fluxes **u** at the internal interfaces of a relaxation subspaces must be zero. So all fluxes remain zero, which is obviously not the solution of the discrete equations. Now what happens if λ^2 is small?

To estimate the convergence rates of the two relaxation methods we use the sup-norm of the residuals $d_a^{(n)}$ and $d_b^{(n)}$ of 3.12a and 3.12b, respectively, after n symmetric Gauss-Seidel sweeps

$$\rho_{SB} = \frac{1}{5} \log \frac{d_b^{(5)}}{d_b^{(10)}} \tag{6.4a}$$

and

$$\rho_V = \frac{1}{5} \log \frac{d_a^{(5)}}{d_a^{(10)}}. \tag{6.4b}$$

Table 6.1 gives the convergence rate ρ_{SB} for superbox-relaxation on a 16×16 grid and different values for λ^2; starting values for ψ and **u** are 0. Table 6.2 gives the convergence rate ρ_V for Vanka-relaxation for the same problem.

TABLE 6.1.
The experimental convergence rate for superbox-relaxation

λ^2	ρ_{SB} lumped	ρ_{SB} non-lumped
10^2	0.403	0.439
10^1	0.080	0.082
10^0	0.037	0.037
10^{-1}	0.032	0.032
10^{-2}	0.031	0.032

TABLE 6.2.
The experimental convergence rate for 5-point Vanka-relaxation

λ^2	ρ_V lumped	ρ_V non-lumped
10^2	2.2357	1.5110
10^1	0.8045	0.7254
10^0	0.6475	0.6368
10^{-1}	0.6317	0.6278
10^{-2}	0.6301	0.6269

From table 6.1 we see that the convergence rate of the superbox-relaxation is small, if $\lambda^2<1$, or equivalently, if the functional F_a^d is only weakly dependent on ψ. The convergence rate of the Vanka relaxation is much larger and less dependent on λ^2.
Lumping appears not to have a strong influence on the convergence rates of both methods.

6.2. A diode problem

As a more relevant testproblem we consider a simple diode (see fig. 6.2). Poisson's equation for the electrostatic potential in this device is

$$\begin{aligned} -\operatorname{div}(\epsilon \operatorname{grad}\psi) + \; & 2n_i q \sinh(\alpha\psi)=D, \quad \text{on } [0,10^{-4}]\times[0,10^{-4}], \\ & 2n_i q \sinh(\alpha\psi)=D, \quad y=0 \vee y=10^{-4}, \\ & \mathbf{u}\cdot\mathbf{n}=0, \quad x=0 \vee x=10^{-4}, \end{aligned} \tag{6.5}$$

$$D(\mathbf{x}) = \begin{cases} +\, qD_0, & y > 0.5\times10^{-4}, \\ 0, & y = 0.5\times10^{-4}, \\ -\, qD_0, & y < 0.5\times10^{-4}. \end{cases} \tag{6.6}$$

Numerical values for the constants appearing in (6.5) and (6.6) are

$$\begin{aligned} \epsilon &= 1.036\times10^{-12}, \\ n_i &= 1.22\times10^{10}, \\ q &= 1.60\times10^{-19}, \\ \alpha &= 38.683, \\ D_0 &= 1.0\times10^{16}. \end{aligned}$$

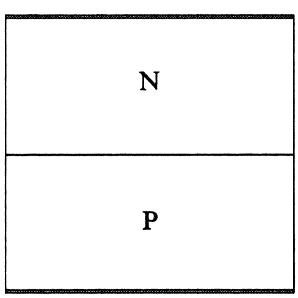

FIGURE 6.2. Configuration of a simple diode.

The minimizing functionals F^d are given by (4.9) with

$$\frac{dR_a}{d\psi} = 2n_i\, q\alpha\psi\cosh(\alpha\psi), \tag{6.7a}$$

$$\frac{dR_b}{d\psi} = 2n_i q \sinh(\alpha\psi), \tag{6.7b}$$

$$R_a(\psi) = n_i q((\psi-\frac{1}{\alpha})e^{\alpha\psi}-(\psi+\frac{1}{\alpha})e^{-\alpha\psi}),$$

$$R_b(\psi) = \frac{2n_i q}{\alpha}\cosh(\alpha\psi). \tag{6.8b}$$

For the above problem we have:

$$2n_i q\alpha = 1.51\times10^{-7}. \tag{6.9}$$

Notice that if we want to compare (6.7a) and (6.2), the values in (6.7a) have to be divided by ϵ. So from (6.9) we conclude that for the superbox-relaxation, no convergence problems are to be expected which are caused by weak dependence of F_a^d on ψ.

However from (6.7) we see that the dependence of $F^d(\psi,\mathbf{u})$ on ψ varies strongly throughout the domain. In the following tables we study how this influences the convergence rates.

Table 6.3 gives values for ρ_{SB} for different grids. In all cases an initial guess was obtained by interpolation from an approximate solution on a coarser grid.

Table 6.4 shows similar data for the Vanka-relaxation method.

TABLE 6.3
The experimental convergence rates for superbox-relaxation

grid	ρ_{SB} lumped	ρ_{SB} non-lumped
8 × 8	0.0199	0.0046
16 × 16	0.0003	0.0007
32 × 32	0.0001	0.0006

TABLE 6.4
The experimental convergence rates for Vanka-relaxation

grid	ρ_V lumped	ρ_V non-lumped
8 × 8	0.3394	0.2330
16 × 16	0.1209	0.0804
32 × 32	0.0693	0.0710

From table 6.3 and 6.4 we see that the convergence rate for Vanka-relaxation is much larger than for superbox-relaxation.

In our experiments with superbox-relaxation we observed that the residuals were locally very large inside the depletion layer between *n*-type and *p*-type material. For an explanation of this slow convergence behaviour consider fig. 6.3.

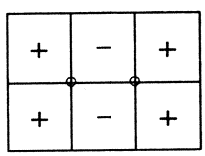

FIGURE 6.3. Dependency of functional F_a^d on ψ.

Suppose that the minimizing functional F_a^d depends weakly on ψ in the middle two cells (indicated by '-'), and strongly in the other 4 cells (indicated by '+'). If the left and middle cells are relaxed, the value of ψ in the middle cells can change considerably, because the functional depends weakly on it; thus leaving a large residual on the interfaces between the middle and right cells. By the same reasoning we find a large residual on the interfaces between the left and middle cells, if the middle and right cells are relaxed. In our diode experiment we observed this wiggling behaviour.

A natural remedy against such behaviour is to use larger relaxation subspaces (e.g. line relaxation)

7. A MULTIGRID METHOD

In order to speed up the convergence of the 5-point Vanka-relaxation we use a Full Approximation Scheme (cf [5]). The advantage of this multigrid method is, that the convergence rates may become mesh-independent. For the relaxation method the convergence rates detoriate on finer meshes (cf. Tables 6.3 and 6.4). In this section some details of our multigrid method are given, and its convergence behaviour is studied by a numerical experiment.

Both pre- and post-relaxation steps in the FAS-algorithm consist of one symmetric Vanka-sweep. The grid transfer operators used, are similar to those given by SCHMIDT and JACOBS [2]. The prolongation, which transfers a solution from a coarse grid to a finer one, is a piecewise constant interpolation for ψ^d, and linear interpolation for $\mathbf{u}^d$. The restriction of the right hand side is defined as the transposed of the prolongation. The restriction of the solution is the weighted average of the fine grid solution.

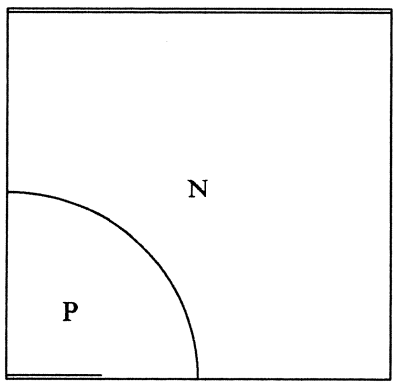

FIGURE 7.1. Quarter circle diode.

To investigate the convergence behaviour of this multigrid method we use a quarter circle diode (see fig. 7.1). The doping profile is defined by

$$D(\mathbf{x}) = \begin{cases} +q.10^{16}, & \|\mathbf{x}\| > 0.5\times10^{-4}, \\ 0, & \|\mathbf{x}\| = 0.5\times10^{-4}, \\ -q.10^{16}, & \|\mathbf{x}\| < 0.5\times10^{-4}. \end{cases} \tag{7.1}$$

The boundary conditions are

$$\begin{aligned} \mathbf{u}\cdot\mathbf{n} = 0, \quad & \text{if } x=0, \\ & x=10^{-4}, \\ & x>0.25\times10^{-4}\wedge y=0, \\ 2n_i q\sinh(\alpha\psi_0)=D, \quad & \text{if } y=10^{-4}, \\ & x<0.25\times10^{-4}\wedge y=0. \end{aligned}$$

The physical constants are as given in section 6.2. The coarsest grid is an uniform 8×8 grid and the coarse grid solution is obtained by relaxation.

Figures 7.2 and 7.3 show the convergence history on different grids for V-cycles, if the discrete equations are lumped, or not lumped, respectively. In both cases we find grid independent convergence, and satisfactory convergence rates.

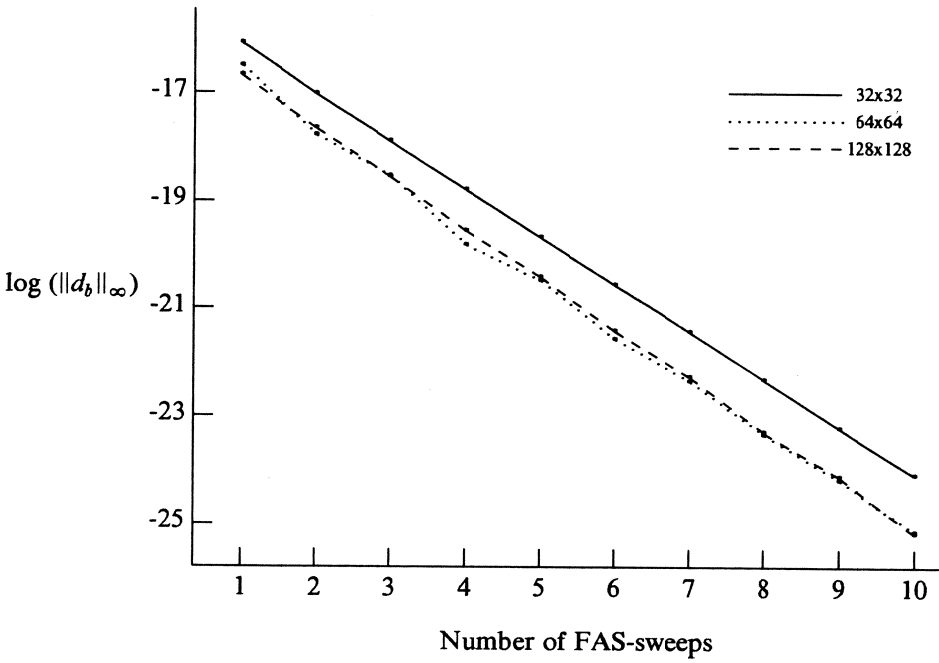

FIGURE 7.2. Convergence history for the quarter circle diode, lumped equations.

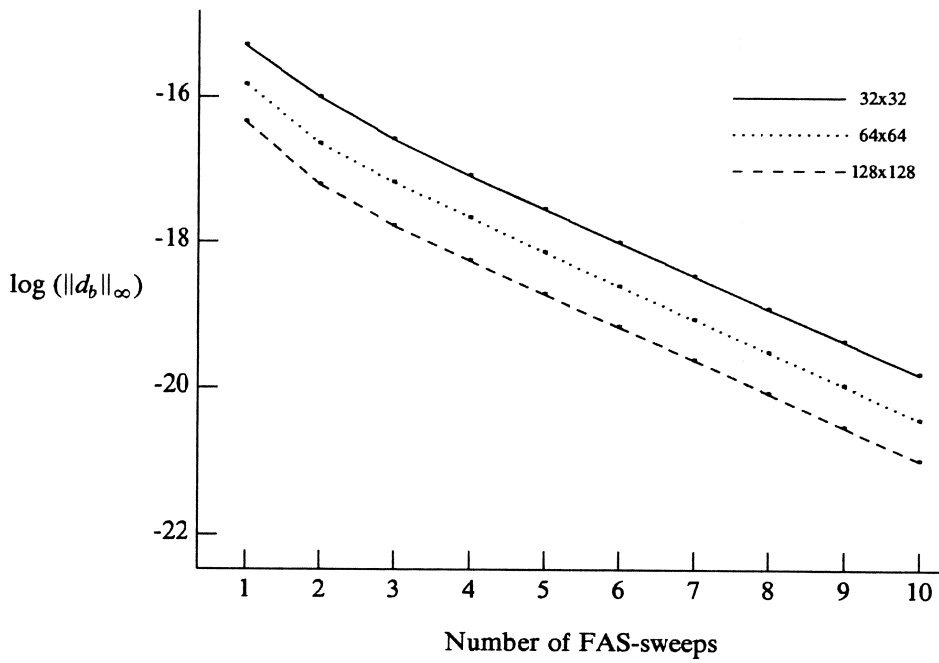

FIGURE 7.3. Convergence history for the quarter circle diode, non-lumped equations.

8. Conclusions

In this paper we have presented two non-linear relaxation methods for a non-linear Poisson equation, with Dirichlet and Neumann boundary conditions. Both relaxation methods are based on minimization of a functional, thus ensuring convergence (cf. Schmidt and Jacobs [2]).

In numerical experiments we observed that, in the presence of Dirichlet boundary conditions, the superbox-relaxation converges slowly if the functional depends weakly on the solution, or if this dependence varies strongly throughout the domain. The Vanka-relaxation gave good results for a simple diode problem. When used as a smoother in a FAS-algorithm we obtained good, grid-independent convergence rates. In the test-problems we studied, lumping was not necessary.

References

1. S.J. Polak, C. Den Heijer, W.H.A. Schilders and P.A. Markovich (1987). *Semi-Conductor Device Modelling from the Numerical Point of View,* Int. J. Numer. Met. Engineering 24, 763-838.
2. G.H. Schmidt and F.J. Jacobs (1988). *Adaptive Local Grid Refinement and Multi-grid in Numerical Reservoir Simulation,* J. Comput. Phys. 77, 140-165.
3. V. Girault and P.A. Raviart (1986). *Finite Element Methods for Navier-Stokes Equations,* Springer-Verlag, Berlin/Heidelberg/New York/Tokyo.
4. S.P. Vanka. *Block-Implicit Multigrid Calculation of Two-dimensional Recirculating Flows,* Comput. Meth. Appl. Mech. Eng. 59 (198), 29-48.
5. A. Brandt (1981). *Guide to Multigrid Development,* Lecture Notes in Mathematics 960, W. Hackbush and U. Trottenberg eds., Springer-Verlag, Berlin, 220-312.